Photochemical Reaction Mechanisms of 2-Nitrobenzyl Compounds in Solution

I. 2-Nitrotoluene: Thermodynamic and Kinetic Parameters of the *aci*-Nitro Tautomer

by **Markus Schwörer** and **Jakob Wirz***

Institut für Physikalische Chemie der Universität Basel, Klingelbergstrasse 80, CH-4056 Basel
(Tel.: +41 61 267 38 42; fax: +41 61 267 38 55; e-mail: J.Wirz@unibas.ch)

Dedicated to Prof. Dr. *Edgar Heilbronner* on the occasion of his 80th birthday

The largely reversible, light-induced tautomerization of 2-nitrotoluene (**1**) to the quinonoid *aci*-nitro tautomer *aci*-**1** was studied by flash photolysis as a benchmark for comparison with the widely used nitrobenzyl phototriggers ('caged compounds'). The pH-rate profile for the decay of *aci*-**1** in aqueous solution exhibits downward curvature at pH 3–4, which is attributed to pre-equilibrium ionization of the nitronic acid *aci*-**1** to its anion $\mathbf{1}^-$ ($pK_a = 3.57$). Two regions of upward curvature, at pH *ca.* 6 and < 0 ($H_0 \approx -1$), each indicate a change in the reaction mechanism. The elementary reactions that dominate between the curved regions are assigned on the basis of kinetic isotope effects and the observation of general acid catalysis: Hydronium ions regenerate 2-nitrotoluene by C-protonation of $\mathbf{1}^-$ in the pH range of 0–6, and H_2O is the proton source at pH > 6. A hird, irreversible *Nef*-type isomerization of *aci*-**1** prevails in highly acidic solutions (pH < 0). The equilibrium constant for the thermal tautomerization of **1** to *aci*-**1** is estimated as $pK_T = 17.0 \pm 0.2$ based on kinetic data.

1. Introduction. – The 2-nitrobenzyl chromophore is widely exploited as a photosensitive protecting group in synthesis [1], photoimaging [2], and for the spatially and temporally controlled release of bioactive compounds such as neurotransmitters or ATP ('caged compounds') [3][4]. Irradiation of 2-nitrobenzyl compounds with at least one H-atom at the benzylic position generates their *aci*-nitro tautomers in the primary photochemical reaction (*Scheme 1*). In the absence of substituents at the benzylic position, the yellow *aci*-nitro compounds revert to the starting materials. Examples of such photochromic [5] behavior are 2-nitrotoluene (**1**) [6], 2,4- and 2,6-dinitrotoluene [7][8], 2,4,6-trinitrotoluene [9], and 2-(2′,4′-dinitrobenzyl)pyridine [10][11]. In the

Scheme 1

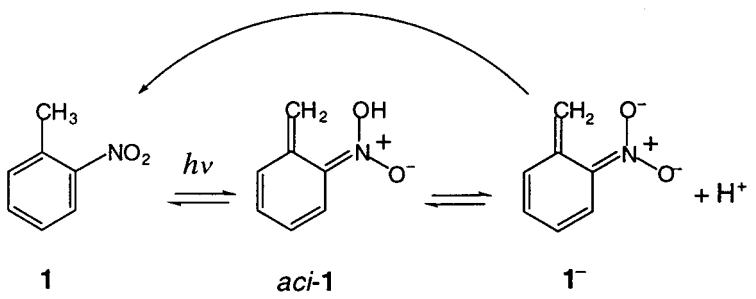

presence of a leaving group at the benzylic position, the *aci*-tautomers form 2-nitrosobenzyl compounds, thereby deprotecting the leaving group.

Reaction rates of the *aci*-nitro intermediates vary strongly with substitution, solvent, and pH. The pattern of these changes is not well understood. In spite of the long-standing interest in the photochemistry of nitrobenzyl compounds, only fragmentary information is available about the efficiency of the primary phototautomerization and about the elementary steps of the subsequent thermal reactions, which eventually lead to deprotection of the caged compounds. The actual release rate, which is essential for time-resolved biochemical applications, is seldom known. For 'caged ATP', the rate constant for the release of ATP in neutral aqueous solution was determined as 90 s^{-1} at 20° [12]. An upper limit of 180 μs was reported for the half-time of Ca^{2+} release from the Ca^{2+} complex of DM-nitrophen (= *N*,*N*′-[1-(4,5-dimethoxy-2-nitrophenyl)ethane-1,2-diyl]bis[*N*-(carboxymethyl)glycine] [13].

In an effort to elucidate the mechanism of photorelease from nitrobenzyl compounds, we have investigated a series of model compounds by flash photolysis. The present, first paper deals with the parent system 2-nitrotoluene (**1**) as a benchmark. The potential-energy surface of **1** and its isomers was recently explored with *ab initio* and density-functional theory [14]. *Wettermark* and co-workers reported the first kinetic studies of the photochromic reaction of **1** in 1962 [6]. We have reinvestigated this reaction in more detail. The elementary reactions of retautomerization that might compete with the release of nitrobenzyl cages were identified. A novel, irreversible reaction was observed in strongly acidic aqueous solutions, and the equilibrium constant between **1** and its *aci*-tautomer was determined.

2. Results. – *Quantum Yields.* Irradiation of **1** in D_2O leads to D-exchange at the benzylic position of **1** [15]. We determined the amount of light-induced D-exchange by GC/MS. A solution of 0.01M NaOH in MeOD was used. Introduction of one D-atom for each molecule of *aci*-**1** formed is assured under these conditions, because **1** is regenerated by deuteron transfer through the solvent (see *Sect. 3*). A stirred solution of **1** (4 ml, 10^{-2}M) was irradiated for 270 s with an excimer laser (351 nm, pulse-repetition rate 3 Hz, pulse energy 81.3 mJ). A quantum yield of *ca.* 0.9% was calculated from the observed amount of D-exchange of 4.31%.

The formation of *aci*-**1** was largely reversible in aqueous solutions at $1 \leq pH \leq 13$, but a minor side reaction led to the disappearance of **1** upon prolonged irradiation. Quantum yields for the disappearance of **1** in various media were estimated spectrophotometrically and are given in *Table 1*. Accurate determination was difficult, because the reaction was inefficient, and the resulting products underwent secondary photolysis. Formation of *aci*-**1** was fully irreversible in strongly acidic aqueous solutions: The quantum yield of disappearance of **1** increased by an order of magnitude at $pH < 0$. UV-Spectral changes suggested formation of 2-nitrosobenzyl alcohol (the characteristic absorption bands of nitrosophenyl compounds at 280 and 320 nm appeared), but proper identification of the photoproduct was inhibited by its instability under the conditions of irradiation.

Primary Photophysical Processes and Formation of aci-**1**. Pump-probe spectroscopy of **1** in MeCN with subpicosecond excitation at 248 nm gave instantaneous (≤ 3 ps) weak transient absorbance in the range of 300 to 600 nm. The absorbances below 360

Table 1. *Quantum Yields ϕ of Disappearance of* **1**[a])

Solvent	ϕ/%
Hexane	0.11
5M $HClO_4/H_2O$	1.73
0.1M $HClO_4/H_2O$	0.20
$3 \cdot 10^{-4}$ M $HClO_4/H_2O$	0.33
$[CH_3COOH]/[CH_3COO^-]$ 0.09M : 0.018M	0.22
H_2O	0.22
$[H_2PO_4^-]/[HPO_4^{2-}]$ 0.025M : 0.025M	0.10
0.1M $NaOH/H_2O$	0.06

[a]) Irradiation at 313 nm.

and above 450 nm decayed with a lifetime of *ca.* 10 ps leaving a persistent Gaussian absorption band, λ_{max} *ca.* 390 nm. The initial diffuse absorbance is tentatively attributed to the excited singlet state of **1** that decays mostly by internal conversion to the ground state, but forms a small amount of *aci*-**1** that persists up to the maximum delay time of 2 ns. Similar absorbance changes were obtained with 2-ethylnitrobenzene (*Fig. 1*). Here, the relative intensity of the persistent absorption by the *aci*-form, $\lambda_{max} \approx 400$ nm, was stronger.

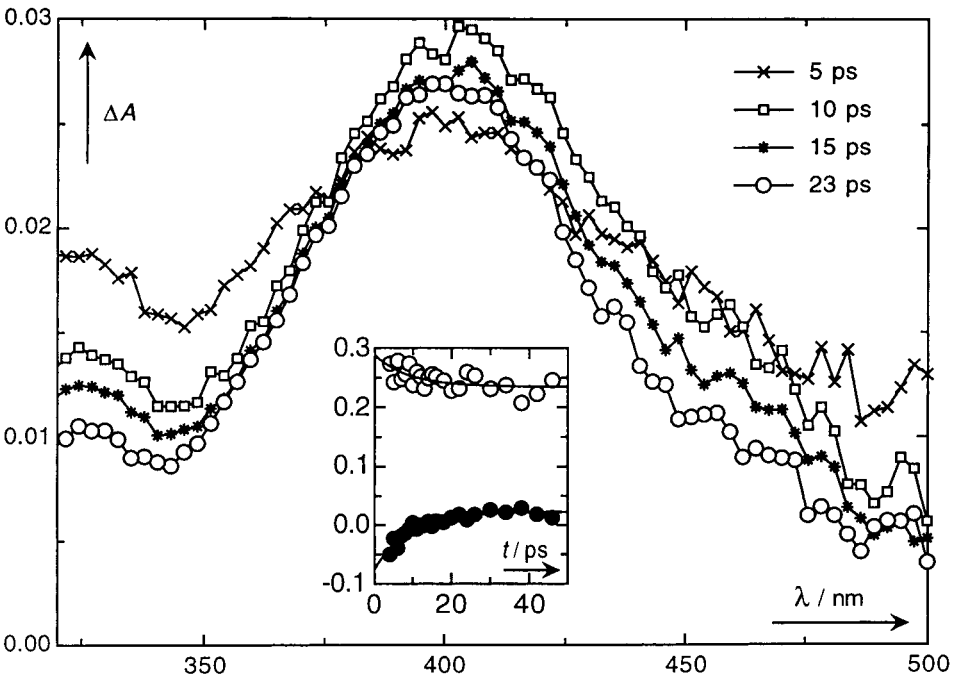

Fig. 1. *Pump-probe spectra observed by subpicosecond excitation of 2-ethylnitrobenzene in acetonitrile. Inset*: Monoexponential functions fitted to the coefficients of the first (○) and second (●) eigenvector determined by global analysis of 26 spectrographic traces, $k = (1.0 \pm 0.3) \cdot 10^{11}$ s^{-1}.

pH-Rate Profile for the Decay of aci-**1** *in Aqueous Solution*. The weak absorption band at λ_{max} *ca.* 390 nm that persists up to 2 ns in the pump-probe spectra of **1** was also observed by nanosecond laser flash photolysis (LFP) of **1** in aqueous solutions. Degassing had no effect on the yield or on the decay kinetics of the transient intermediate. The absorption maximum of the transient shifted from 390 nm in acidic aqueous solutions to 405 nm in neutral or basic solutions. These absorptions are assigned to the neutral and ionized forms of the quinonoid tautomer of **1**, *aci*-**1**, and $\mathbf{1}^-$ (*Scheme 1*), respectively, in agreement with *Wettermark* and co-workers [6]. In neutral, unbuffered solutions, the absorbance shift accompanying ionization of *aci*-**1** was resolved in time by nanosecond LFP: The absorbance on the blue edge of the band (365 nm) initially showed partial decay with a rate constant of *ca.* $2 \cdot 10^7\ s^{-1}$. A corresponding growth in absorbance was observed at 410 nm (*Fig. 2*). In solutions containing buffers or base, the ionization equilibrium *aci*-$\mathbf{1} \rightleftharpoons \mathbf{1}^- + H^+$ was established within the 25-ns duration of the excitation pulse. Transient decays monitored at 405 nm obeyed first-order kinetics accurately, with rate constants k_{obs} depending on pH and on buffer concentrations. We did not encounter the biphasic decays in AcOH buffer solutions that were reported by *Wettermark* and co-workers [6]. The pH-rate profile for the decay of *aci*-**1** is shown in *Fig. 3*, the data are given in *Table 2*. Nonlinear least-squares fitting of *Eqn. 1* to the data points provided the rate coefficients k_0', k_{H^+}', k_{H^+}, and the ionization quotient of *aci*-**1**, $K_{a,c}$, given in *Table 3*. *Eqn. 1* is derived in *Sect. 3*. Rate coefficients are dashed (*e.g.*, k_0') when they refer to an elementary reaction involving the anion $\mathbf{1}^-$.

$$\log (k_{obs}/s^{-1}) = \log [\{(k_0' + k_{H^+}' [H^+])\ K_{a,c} + k_{H^+}[H^+]^2\}/\{(K_{a,c} + [H^+])s^{-1}\}] \qquad (1)$$

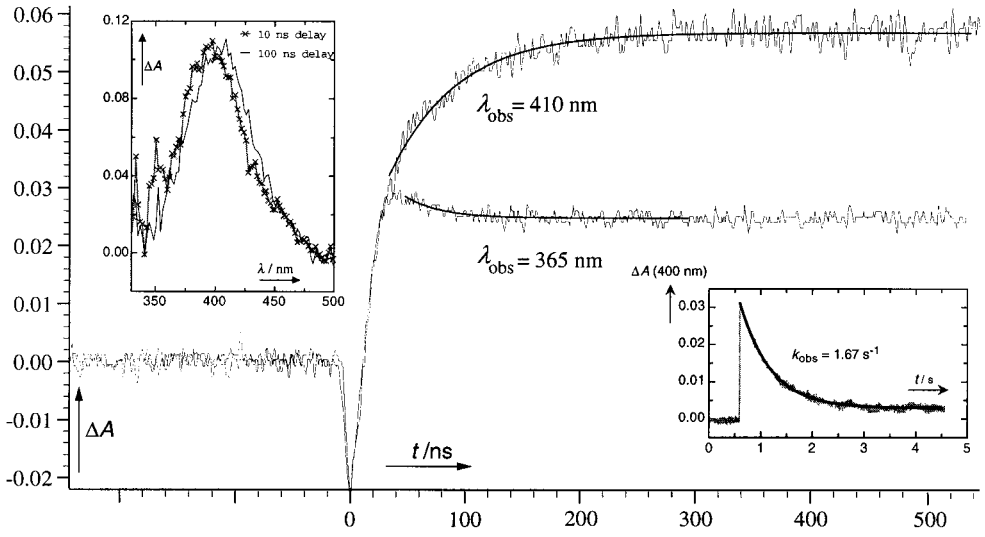

Fig. 2. *Deprotonation of* aci-**1** *in unbuffered water*. The inset on the left shows transient spectra recorded by nanosecond LFP (excitation at 248 nm, pulse width 25 ns, pulse energy 100 mJ). The inset on the right shows the decay kinetics of $\mathbf{1}^-$.

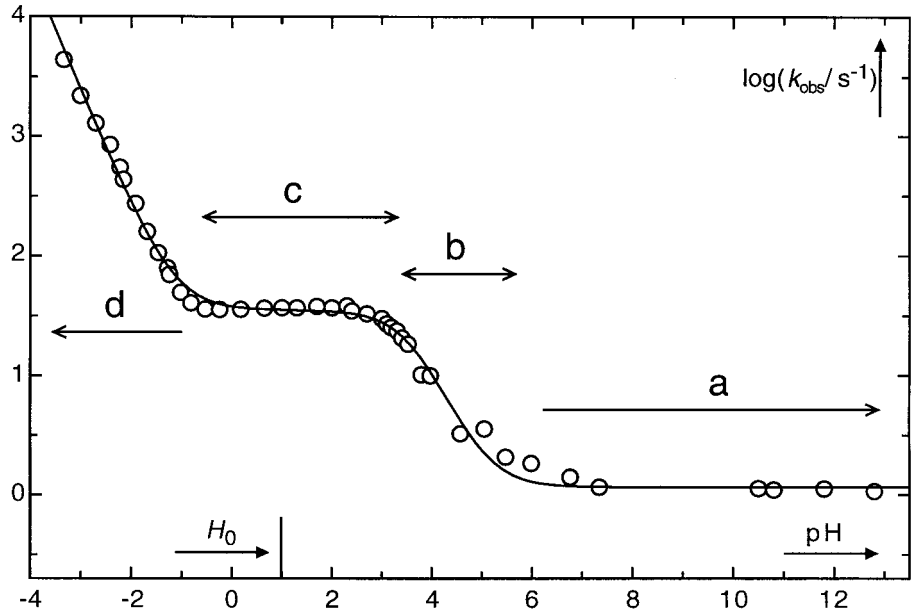

Fig. 3. *pH-Rate profile for the decay of* aci-**1**. The solid line was obtained by nonlinear least-squares fitting of *Eqn. 1*. The regions labeled 'a' – 'd' are addressed in *Sect. 3*.

Kinetics in Nonaqueous Solvents. Ionization of *aci*-**1** was resolved by LFP in several polar solvents. The rate constants are given in *Table 4*. *aci*-**1** did not ionize in hexane, 1,1,1-trifluoroethanol, CH_2Cl_2, CCl_4, and dry DMSO. Addition of NaOH accelerated the deprotonation, whereas addition of $HClO_4$ suppressed it.

In most nonaqueous solvents, the decay of the *aci*-nitro transient was biexponential (*Table 4*). The absorption maximum of the fast component, which is attributed to the (*Z*)-isomer of *aci*-**1**, was at slightly longer wavelength (λ_{max} *ca.* 405 nm in hexane) than that of the slow component due to (*E*)-*aci*-**1** (λ_{max} *ca.* 380 nm). In MeCN and protic solvents, the equilibrium between these two isomers is established rapidly by proton transfer through the solvent, and the *aci*-decay obeys a single exponential rate law.

Solutions of **1** and D_7-**1** in hexane with matched absorbances were flashed with an excimer laser (248 nm, 200 mJ, $24 \pm 1°$). The amplitudes of both the fast (*Z*) and the slow (*E*) components of the *aci*-transient were lower by a factor of *ca.* 3 in the perdeuterated compound. The kinetic isotope effect on the fast-decaying component was $k_H/k_D = 1.87 \pm 0.14$ (4 measurements).

Thermal Isotope Exchange and Determination of the CH Acidity Constant of **1**. The 2-nitrotoluene (**1**) is a weak C-acid that does not ionize noticeably in aqueous base. The ionization constant of **1** was, therefore, determined kinetically. Deprotonation of **1** to $\mathbf{1}^-$ in the ground state was measured by monitoring base-catalyzed isotopic substitution of the methyl H-atoms of **1** in 1N NaOD at $25 \pm 0.1°$. Three runs were analyzed at low conversion by GC/MS analysis (see *Exper. Part*). Rate constants k_{DO^-} for base-catalyzed deuteration of **1** were determined for each run by assuming a first-order rate law for single deuteration of **1**, $[D_1\text{-}\mathbf{1}]_t/[\mathbf{1}]_{t=0} = 1 - \exp(-k_{DO^-}[DO^-]t)$, which gave an

Table 2. pH-*Dependent Rate Constants* k_{obs} *and Buffer Slopes* k_{buffer} *of the Decay of* aci-**1** *in Aqueous Solution at* $25 \pm 0.1°$ [a])

Acid/base	Buffer ratio	Conc./M	pH[b])	k_{obs}/s^{-1}	$k_{buffer}/(M^{-1}\ s^{-1})$	Number of runs
$HClO_4$		6.825	−3.33	4370 ± 70		4
$HClO_4$		6.338	−3.00	2190 ± 10		4
$HClO_4$		5.85	−2.70	1290 ± 26		7
$HClO_4$		5.363	−2.42	851 ± 11		4
$HClO_4$		5.00	−2.22	550 ± 11		3
$HClO_4$		4.875	−2.16	433 ± 8		6
$HClO_4$		4.388	−1.92	272 ± 5		5
$HClO_4$		3.900	−1.69	159 ± 1		4
$HClO_4$		3.413	−1.47	106 ± 1		6
$HClO_4$		3.000	−1.28	79.0 ± 2.4		3
$HClO_4$		2.925	−1.25	70.0 ± 0.5		7
$HClO_4$		2.438	−1.03	49.5 ± 0.3		4
$HClO_4$		2.00	−0.82	40.5 ± 0.1		3
$HClO_4$		1.463	−0.53	35.9 ± 0.3		3
$HClO_4$		1.00	−0.25	35.6 ± 0.1		4
$HClO_4$		0.500	0.18	35.8 ± 0.2		3
$HClO_4$		0.200	0.65	36.6 ± 0.3		5
$HClO_4$		0.100	1.00	36.9 ± 0.2		3
$HClO_4$		0.050	1.30	36.9 ± 0.4		4
$HClO_4$		0.020	1.70	38.0 ± 0.2		5
$HClO_4$		0.010	2.00	36.9 ± 0.1		5
$HClO_4$		0.005	2.30	38.4 ± 0.2		4
$HClO_4$		0.004	2.40	34.8 ± 0.3		4
$HClO_4$		0.002	2.70	32.9 ± 0.5		4
$HClO_4$		0.001	3.00	30.0 ± 0.3		4
$HClO_4$		0.008	3.10	27.1 ± 0.1		4
$HClO_4$		0.00065	3.19	25.3 ± 0.1		4
$HClO_4$		0.0005	3.30	23.6 ± 0.1		4
$HClO_4$		0.0004	3.40	20.7 ± 0.1		3
$HClO_4$		0.0003	3.52	18.4 ± 0.2		5
AcOH/NaOAc	6.00	0.02 – 0.23	3.79	10.2 ± 3.4	1170 ± 60	5
AcOH/NaOAc	4.00	0.005 – 0.10	3.97	10.0 ± 0.1	1080 ± 2	5
AcOH/NaOAc	1.00	0.002 – 0.16	4.57	3.27 ± 0.22	811 ± 19	6
AcOH/NaOAc	0.333	0.002 – 0.11	5.05	3.59 ± 0.13	405 ± 12	7
AcOH/NaOAc	0.125	0.005 – 0.113	5.47	2.08 ± 0.04	174 ± 2	5
$H_2PO_4^-/HPO_4^{2-}$	6.00	0.016 – 0.078	6.00	1.84 ± 0.18	270 ± 4	4
$H_2PO_4^-/HPO_4^{2-}$	1.00	0.002 – 0.05	6.78	1.41 ± 0.11	174 ± 4	5
$H_2PO_4^-/HPO_4^{2-}$	0.333	0.004-0.04	7.36	1.16 ± 0.04	102 ± 2	4
NaOH		0.0005	10.50	1.13 ± 0.01		4
NaOH		0.001	10.80	1.10 ± 0.01		4
NaOH		0.010	11.80	1.12 ± 0.02		5
NaOH		0.100	12.80	1.07 ± 0.01		4

[a]) Aqueous solutions of pH ≥ 1 were prepared by addition of 1% by volume from an EtOH stock solution of **1**.
[b]) In the range of $1 \leq pH \leq 13$, ionic strength was adjusted to $I = 0.1$M by addition of $NaClO_4$. The pH values given for aqueous acid refer to nominal concentrations of $HClO_4$. At concentrations of $HClO_4$ exceeding 0.1M, *Hammett*'s acidity scale H_0 was used [16]. Proton concentrations in aqueous NaOH solutions were calculated from the nominal concentrations of OH^- using the dissociation quotient of H_2O at ionic strength $I = 0.1$M, $K_{w,c} = 1.59 \cdot 10^{-14}$ M^2 [17]. Proton concentrations of AcOH buffers were calculated using an ionization quotient, $pK_{a,c} = 4.57$, which was calculated from the thermodynamic acidity constant $pK_a^o = 4.76$ [18] and activity coefficients recommended by *Bates* [17] ($I = 0.1$M). Similarly, the thermodynamic acidity constant for KH_2PO_4 ($pK_a^o = 7.21$ [19]) gave the ionization quotient $pK_{a,c} = 6.78$ ($I = 0.1$M) to calculate proton concentrations in phosphate buffers. Rate constants determined with buffer solutions were extrapolated to zero buffer concentration.

Table 3. *Kinetic and Thermodynamic Parameters*[a])

	Reaction	Value
k_{-H^+}	*aci*-**1** $\rightarrow$ **1**$^-$ + H^+	*ca.* $2 \cdot 10^7$ s^{-1}
k_0'	**1**$^-$ + $H_2O \rightarrow$ **1** + OH^-	1.16 ± 0.03 s^{-1}
k_{H^+}	*aci*-**1** + $H^+ \rightarrow$ nitroso compound	(2.47 ± 0.05) M^{-1} s^{-1}
k_{H^+}'	**1**$^-$ + $H^+ \rightarrow$ **1**	$(1.26 \pm 0.09) \cdot 10^5$ M^{-1} s^{-1}
$pK_{a,c}$(*aci*-**1**)	*aci*-**1** $\rightleftarrows$ **1**$^-$ + H^+	3.57 ± 0.02
$pK_{a,c}$(**1**)	**1** $\rightleftarrows$ **1**$^-$ + H^+	20.6 ± 0.2

[a]) Aqueous solutions, T 298 K, ionic strength $I = 0.1$M.

average of $k_{DO^-} = (3.1 \pm 0.09) \cdot 10^{-7}$ M^{-1} s^{-1}. The rate constant of the reverse reaction, C-protonation of **1**$^-$ by water in 1M NaOH was determined by LFP, $k_0' = 1.07 \pm 0.02$ s^{-1}. Ignoring kinetic isotope effects, the concentration quotient for deprotonation of **1** by hydroxide ion was estimated as $K_c \approx k_{DO^-}/k_0' = 2.9 \cdot 10^{-7}$M^{-1}.

The rate of deprotonation of **1** by hydroxide ion in H_2O, k_{HO^-}, differs from k_{DO^-} by a solvent isotope effect, k_{HO^-}/k_{DO^-}, which can be estimated with sufficient accuracy. It depends on the fractional extent x of proton transfer in the transition state (see *Eqn. 2*) [20]. According to *Eqn. 2*, the solvent isotope effect will decrease from unity for very strong acids (early transition state, $x \rightarrow 0$) to 1/2.4 for very weak acids (late transition state, $x \rightarrow 1$). *Kresge* has shown that x may be identified with the fraction of the total-energy change that the system undergoes in passing from reactants through the transition state to products (see *Eqn. 3*) [21]. Kinetic isotope effects for the ionization

Table 4. *Rate Constants of Ionization and Retautomerization of* aci-**1** *in Various Nonaqueous Solvents*

Solvent	*aci*-**1** decay		*aci*-**1** dissociation	**1**$^-$ decay
	fast k/s^{-1}	slow k/s^{-1}	k_{-H^+}/s^{-1}	k_0'/s^{-1}
Hexane, dried over mol. sieve	$(1.2 \pm 0.1) \cdot 10^5$	18.6 ± 1.3		
Hexane	$(5.3 \pm 0.2) \cdot 10^5$	18		
Hexane, H_2O-saturated	$(8.4 \pm 0.4) \cdot 10^5$	18 ± 1		
1,1,1-Trifluorethanol	$(2.2 \pm 0.1) \cdot 10^5$	1.5		
0.1% H_2O/DMSO	$(1.0 \pm 0.1) \cdot 10^6$	6.7		
H_2O/DMSO 35 : 65			$3 \cdot 10^3$	$1 \cdot 10^2$
DMF	$(4.8 \pm 1.6) \cdot 10^5$		$6 \cdot 10^3$	$3.5 \cdot 10^2$
HMPA (dist. over BaO)			$6 \cdot 10^3$	$2.6 \cdot 10^2$
0.02% H_2O/MeCN			$2.6 \cdot 10^5$	$8 \cdot 10^3$
1% H_2O/MeCN			$4.9 \cdot 10^5$	$1.7 \cdot 10^2$
1% 1M NaOH/MeCN			$5.6 \cdot 10^5$	7
0.1% 1M HCl/MeCN		5.18		
CCl_4	$(4.5 \pm 0.3) \cdot 10^5$	14.4		
CH_2Cl_2	$(1.3 \pm 0.1) \cdot 10^5$	24.1		
EtOH, 96%			$1 \cdot 10^4$	$4.4 \cdot 10^2$
EtOD, abs.			$6 \cdot 10^3$	70
0.5% 0.1M $HClO_4$/MeOH	$4.74 \cdot 10^6$	1.41		
MeOH	$(2.3 \pm 0.3) \cdot 10^5$		$1 \cdot 10^4$	$(5.3 \pm 0.6) \cdot 10^2$
0.5% 0.01M NaOH/MeOH	$(2.0 \pm 0.1) \cdot 10^5$		$2.5 \cdot 10^4$	$5.52 \cdot 10^2$
1% 1M NaOH/MeOH			$4.5 \cdot 10^7$	$5.31 \cdot 10^2$

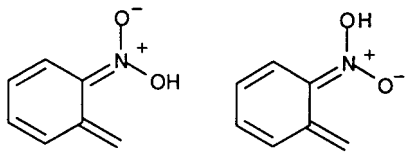

(*Z*)-*aci*-**1** (*E*)-*aci*-**1**

of nitroalkanes were predicted to lie in the range of $k_{HO^-}/k_{DO^-} = 0.69 \pm 0.01$, in excellent agreement with experimental data.

$$k_{HO^-}/k_{DO^-} = (1/2.4)^x \tag{2}$$

$$x = \Delta G^{\neq}/(2\Delta G^{\neq} - \Delta G^{o}) \tag{3}$$

To determine x for the reaction $\mathbf{1} + HO^- \rightarrow \mathbf{1}^- + H_2O$, we required the standard free energies of reaction, ΔG^o, and of activation, $\Delta G^{\neq}$: $\Delta G^o = -RT \ln\{K_c/(\sigma M^{-1})\} \approx 40$ kJ mol^{-1} (symmetry factor $\sigma = 3$, $K_c \approx k_{DO^-}/k_0' = 2.9 \cdot 10^{-7} M^{-1}$), $\Delta G^{\neq} \approx -RT \ln\{hk_{DO^-}/(k_B T \sigma M^{-1})\} = 113$ kJ mol^{-1}. We obtained $x = 0.61$ from *Eqn. 3* and, hence, $k_{HO^-}/k_{DO^-} = 0.59$ from *Eqn. 2*. We consider this value to be accurate within $\pm 10\%$. It is somewhat smaller than the value of 0.69 determined for nitroalkanes, because **1** is a weaker acid. The rate constant for deprotonation of **1** in 1M aqueous base was then calculated as $k_{HO^-} = (1.8 \pm 0.6) \cdot 10^{-7} M^{-1}$ s^{-1}. The ratio $k_{HO^-}/k_0' = (1.7 \pm 0.6) \cdot 10^{-7} M^{-1}$ is equal to the concentration quotient K_c ($I = 1M$) for the deprotonation reaction $\mathbf{1} + HO^- \rightarrow \mathbf{1}^- + H_2O$. We assume that K_c does not depend on ionic strength, because it refers to a charge-shift reaction. With $K_w(I = 0.1M) = 1.59 \cdot 10^{-14} M^2$ [17] for the ionization quotient of water, the ionization quotient of **1** as a C-acid at ionic strength $I = 0.1M$ was then calculated as $K_{a,c}(\mathbf{1}) = (k_{HO^-}/k_0')K_w = (1.7 \pm 0.6) \cdot 10^{-7} \cdot (1.59 \cdot 10^{-14})$ $M = (2.7 \pm 1.0) \cdot 10^{-21}$ M, $pK_{a,c}(\mathbf{1}) = 20.6 \pm 0.2$ ($I = 0.1M$).

Extrapolation of acidity constants determined in DMSO/H_2O mixtures to wholly aqueous solution gave $pK_a(\mathbf{1}) > 25$ which, from the present data, appears to be too high [22]. Solvent isotope effects on the decay rate constants of *aci*-**1** in H_2O and D_2O (*Fluka*, 99.9%) solutions are given in *Table 5*.

3. Discussion. – *Quantum Yield of* aci-**1** *Formation*. The phototautomerization of **1** to *aci*-**1** is inefficient. *Margerum* and *Petrusis* [23] compared the intensity of the transient absorption obtained by the photodecarboxylation of 2-nitrophenyl acetate, an irreversible reaction proceeding *via aci*-**1**, with that obtained by flash photolysis of **1**. They estimated the quantum yield for the formation of *aci*-**1** from **1** in aqueous solution at pH 10 as $\phi_{aci\text{-}1} \approx 1\%$. From the quantum yield of photodeuteration determined in this work, we obtained a similar value, $\phi_{aci\text{-}1} \approx 0.9\%$. Formation of *aci*-**1** was not fully reversible. Quantum yields for the disappearance of **1** under various conditions were around $\phi_{dis} \approx 0.2\%$ (*Table 1*). *Simmons* and *Zepp* [24] have reported a $\phi_{dis} = (2.2 \pm 0.4) \cdot 10^{-3}$ for 366-nm irradiation of **1** in aqueous solution at pH 5.5.

Table 5. *Solvent Deuterium Isotope Effects*[a])

Solvent[a]) L = H or D	k_H/s^{-1} (number of measurements)	k_D/s^{-1} (number of measurements)	k_H/k_D
5.125M $LClO_4/L_2O$	457 ± 21[b])	1989 ± 99 (3)	0.23 ± 0.02
0.2M $LClO_4/L_2O$	36.6 ± 0.5 (5)	7.18 ± 0.05 (5)	5.1 ± 0.1
0.1M NaOL/L_2O	1.07 ± 0.02 (4)	0.149 ± 0.02 (4)	7.2 ± 0.2
0.01M NaOL in MeOL	530 ± 14 (5)	68.7 ± 4.8 (8)	7.8 ± 0.6

[a]) Basic solutions in D_2O were prepared by diluting a solution of 40% NaOD in D_2O, basic methanol solutions by dissolving solid NaOH in MeOD. Concentrated acidic solutions were made from 70% $DClO_4$ in D_2O; dilute aqueous acid solutions (up to 0.2M) were made by adding the appropriate amount of concentrated $HClO_4$ (70%) to D_2O. Except for the measurements in 5.125M perchloric acids (room temperature, $24 \pm 1°$), all samples were thermostatted at $25 \pm 0.1°$. [b]) Calculated from parameters determined by fitting of *Eqn. 1*. The error is an average of errors of measurements in 5.363, 5.00, and 4.875M $HClO_4$.

Subpicosecond Spectroscopy of **1**. Several groups have studied the primary photophysical processes of nitrobenzene and 2-nitrotoluene (**1**). The triplet yield of nitrobenzene was determined as 0.67 ± 0.10 by energy-transfer experiments [25] and, more recently, as ≥ 0.8 by a transient-grating method [26]. In the latter study, the triplet yield of **1** was determined as 0.79 ± 0.04 in both EtOH and hexane. The lifetimes of the triplet states were found to be 480 ± 50 ps for nitrobenzene and 350 ± 50 ps for **1** in EtOH at room temperature. $S_1 - T_1$ Intersystem crossing of nitrobenzene was tentatively attributed to a process with 6 ps lifetime that was observed by a population-grating technique [27]. Broad transient absorptions in the visible region, λ_{max} *ca.* 440 and 630 nm, were observed by pump-probe spectroscopy of nitrobenzene and of **1**, and were attributed to triplet-triplet absorptions, which rose within ≤ 5 ps and decayed with lifetimes of the order of 700 ps [28].

The pump-probe experiments reported in this work did not provide any evidence for intersystem crossing to the triplet state of **1**. The observations were consistent with predominant internal conversion of the excited singlet state. 'Aborted' H-transfer [29] may be responsible for this fast process. More important, the present pump-probe experiments established that formation of the phototautomer *aci*-**1** was complete within *ca.* 10 ps of excitation and that *aci*-**1** persisted for up to 2 ns. The low quantum yield of *aci*-formation observed by nanosecond LFP can not be attributed to a fast retautomerization of the (*Z*)-isomer.

Analysis of the pH-Rate Profile for the Decay of aci-**1** *in Aqueous Solution*. The pH dependence shown in *Fig. 3* exhibits two regions of acid-catalyzed decay (marked 'b' and 'd') and two pH-independent regions ('a' and 'c'). The two intermediate, upward-bent regions, at $H_0 = -1$ connecting 'c' and 'd' and at $pH \approx 6$ connecting 'a' and 'b', indicate a change in the dominant reaction mechanism [30][31], namely from a pH-independent mechanism to an acid-catalyzed one, as the acidity is increased. Therefore, three independent reaction mechanisms need to be identified.

We begin with the pH-independent region 'a' at $pH > 6$, where the *aci* transient is fully ionized to $\mathbf{1}^-$. The only conceivable process for the decay of $\mathbf{1}^-$ in this region is protonation of $\mathbf{1}^-$ by solvent water (see *Eqn. 4*). Intramolecular cyclization of $\mathbf{1}^-$ to a dihydrobenzisoxazole anion faces a prohibitive barrier [14] and would not show a primary kinetic isotope effect. The large primary kinetic isotope effect observed in 0.1M

NaOH/NaOD, $k_H/k_D = 7.16 \pm 0.17$, confirms that the rate-determining step is C-protonation of $\mathbf{1}^-$ by solvent water.

$$\mathbf{1}^- + H_2O \rightarrow \mathbf{1} + HO^- \quad (4)$$

Acid catalysis becomes noticeable below pH 6 (region 'b'), and saturates at pH 4, as the second pH-independent region 'c' is approached. The downward curvature connecting regions 'b' and 'c' at pH *ca.* 3.5 is attributed to rapid equilibration between the nitronic acid *aci*-**1** and its anion $\mathbf{1}^-$. Dissociation of *aci*-**1** to $\mathbf{1}^-$ results in a long-wavelength shift of the transient absorption spectrum in solutions with pH > 3.6. Moreover, the ionization process itself was directly observed in neutral water with a rate constant k_{-H^+} of *ca* $2 \cdot 10^7$ s^{-1} in the absence of buffers (*Fig. 2*). The ratio k_{-H^+}/k'_{H^+} must be equal to the acidity constant, $K_{a,c}$(*aci*-**1**) $= 2.71 \cdot 10^{-4}$ M (*Table 3*), and this determines the rate constant for O-protonation of $\mathbf{1}^-$, $k'_{H^+} = 7.4 \cdot 10^{10}$ M^{-1} s^{-1}. This value is close to the diffusion-controlled limit, as expected. Note that the ionization rate of $2 \cdot 10^7$ s^{-1} (or faster, in the presence of buffers) ensures rapid equilibration between the (*E*)- and (*Z*)-isomers of *aci*-**1** by proton exchange through the solvent water.

The reaction mechanism does not change in the downward-bent region connecting 'b' and 'c' [30][31]. Three elementary processes may be considered for the decay of the *aci*-tautomers in the region 'b – c'. *i*) Intramolecular cyclization reaction of *aci*-**1** could form a non-absorbing dihydrobenzisoxazole intermediate, which eventually regenerates **1**. The barrier for cyclization of *aci*-**1** was calculated as 77 kJ mol^{-1}, much lower than that for cyclization of $\mathbf{1}^-$, 164 kJ mol^{-1} [14]. Cyclization of *aci*-**1**, but not of $\mathbf{1}^-$, could explain the shape of the pH profile in the region 'b – c'. Such a mechanism can, however, be excluded on the basis of the observed deuterium isotope effect, $k^H_{obs}/k^D_{obs} = 5.1 \pm 0.1$ in 0.2M $LClO_4$ (L = H, D). Cyclization of *aci*-**1** in region 'c' would not be subject to a primary kinetic isotope effect.

ii) Intramolecular proton transfer from the nitronic acid function of *aci*-**1** to the methylene C-atom is excluded by the observation of general acid catalysis in AcOH and phosphate buffers (*vide infra*). The rate of intramolecular proton transfer would only exhibit specific acid catalysis, because H^+ concentration determines the ionization ratio of *aci*-**1**.

iii) We are left with a rate-determining protonation of the methylene C-atom of $\mathbf{1}^-$ by H^+ according to *Scheme 2* as the only conceivable reaction mechanism prevailing in regions 'b' and 'c'. This mechanism accounts both for general acid catalysis and for the observed kinetic isotope effect of $k^H_{obs}/k^D_{obs} = 5.1$ in region 'c'. *Eqn. 5* gives the rate law derived from the mechanism of *Scheme 2* in the absence of general acids, where $[aci\text{-}\mathbf{1}]_t = [aci\text{-}\mathbf{1}] + [\mathbf{1}^-]$ is the total concentration of the *aci*-nitro tautomer. The right-hand expression of *Eqn. 5* is obtained by substituting the variable $[\mathbf{1}^-]$ by $[aci\text{-}\mathbf{1}]_t$ using the ionization quotient of *aci*-**1**, $K_{a,c} = [H^+]\ [\mathbf{1}^-]/[aci\text{-}\mathbf{1}]$. The isotope effect was measured in 0.2M $LClO_4$ where $[L^+] \gg K_{a,c}$, so that *Eqn. 5* simplifies to *Eqn. 6*.

$$-d[aci\text{-}\mathbf{1}]_t/dt = k'_{H^+}\ [\mathbf{1}^-]\ [H^+] = k'_{H^+}\ K_{a,c}\ [aci\text{-}\mathbf{1}]_t\ [H^+]/([H^+] + K_{a,c}) \quad (5)$$

$$-d[aci\text{-}\mathbf{1}]_t/dt = k'_{H^+} K_{a,c} [aci\text{-}\mathbf{1}]_t \quad (6)$$

The observed solvent isotope effect is, therefore, composed of a primary isotope effect on the protonation rate constant k'_{H^+} and a solvent isotope effect on the acidity constant of *aci*-**1**, $K_{a,c}$ (see *Eqn. 7*).

$$k_{obs}^{H}/k_{obs}^{D} = (k'_{H^+}/k'_{D^+})(K_{a,c}^{H_2O}/K_{a,c}^{D_2O}) \quad (7)$$

With $K_{a,c}^{H_2O}/K_{a,c}^{D_2O} \approx 1/3$ [32], we obtain $k'_{H^+}/k'_{D^+} \approx 5.1/3 = 1.7$ for the primary kinetic isotope effect on the protonation of $\mathbf{1}^-$, which is much smaller than that observed in 0.1M NaOL for the protonation of $\mathbf{1}^-$ by water. The reduction may be attributed to the high free energy of proton transfer in the second step of *Scheme 2*. Primary kinetic isotope effects of C-protonation reach their maximum only when the fractional extent of proton transfer in the transition state is close to 0.5, see, *e.g.*, [33].

Scheme 2

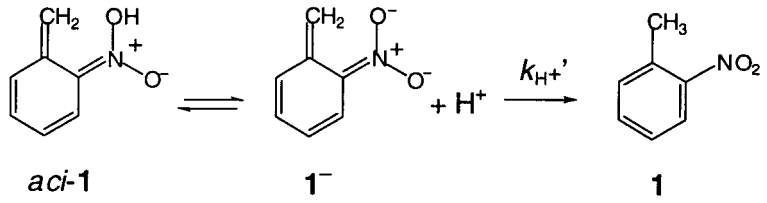

Moving to strongly acidic solutions ($pH < 0$), we encounter a second positive curvature connecting the plateau 'c' to the region 'd' of acid catalysis. At the same time, the largely photochromic (reversible) photoreaction of **1** becomes irreversible. (The same effect is observed in MeOH solution as perchloric-acid concentrations exceed 0.01M). The formation of a new product excludes C-protonation of *aci*-**1** as the mechanism prevailing in region 'd', which would amount to regeneration of **1**. Formation of the photoproduct can be monitored at 320 nm. The rate constant of the absorbance growth at this wavelength is the same as that for the decay of *aci*-**1** observed at 390 nm for acid concentrations exceeding 1M. UV Spectra of irradiated solutions of **1** in perchloric-acid solutions (> 1M) and MeOH solutions containing 0.1M perchloric acid suggest formation of 2-nitrosobenzyl alcohol, which is, however, not stable under these conditions. Absorption bands and photoinstability of the new product are comparable to those of related nitroso aromatics, *e.g.*, 2-nitrosobenzaldehyde.

In region 'd', the kinetic isotope effect becomes strongly inverse, $k_{H^+}/k_{D^+} = 0.23 \pm 0.02$ in 5.125M $LClO_4$ ($H_0 = -2.29$), which provides strong evidence that a fast protonation equilibrium precedes the rate-determining step. At such high acid concentrations, further protonation of *aci*-**1** to the diprotonated cation *aci*-$\mathbf{1}^+$ is likely (*Scheme 3*). Protonation of nitronic acids is assumed to be a key step in the *Nef* reaction [34–36] and in the *Meyer* reaction [37][38], as well as in acid-catalyzed aromatic substitution reactions of nitromethanes [39].

The positively charged benzylic C-atom of *aci*-$\mathbf{1}^+$ should be prone to nucleophilic attack by water to form the nitroso hydrate **2**. *Grünbein et al.* [40] have investigated the dehydration reaction of aromatic nitroso hydrates to the corresponding nitroso compounds. Their results show that a rapid protonation preequilibrium is followed by

Scheme 3. *Proposed Mechanism for the Irreversible Photodecomposition of* **1** *in Aqueous* $HClO_4$ *Solution*

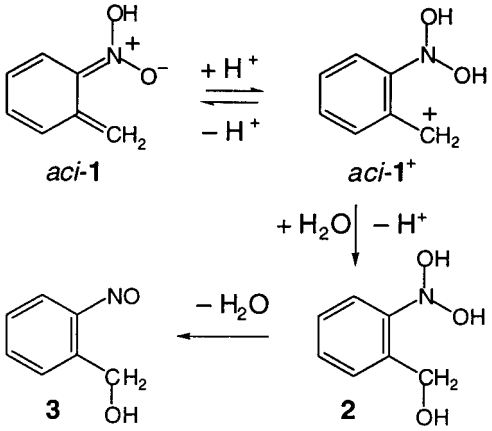

slow dehydration, and that the nitroso hydrate does not absorb at 320 nm. A rate constant for dehydration, $k = 1.2 \cdot 10^4\ s^{-1}$ at $H_0 < -0.5$, and a pK_a of 0.4 ± 0.2 were reported for 3-nitrosotoluene hydrate. From these data, the dehydration step $\mathbf{2} \rightarrow \mathbf{3} + H_2O$ (*Scheme 3*) is expected to be much faster than the observed rate constant for the disappearance of *aci*-**1** at pH < 1. The rate of the rate-determining hydration reaction is expected to be proportional to $[H^+]$ as long as $pK_a(aci\text{-}\mathbf{1}^+) < H_0$. As proton catalysis in strong acids does not saturate down to $H_0 = 3$, the pK_a of *aci*-$\mathbf{1}^+$ must be below -3. Thus, rate-determining water attack on *aci*-$\mathbf{1}^+$ explains both the inverse kinetic isotope effect on the decay of *aci*-**1** and the equal rate constants for the decay of *aci*-**1** and for the formation of the photoproduct observed at 320 nm.

Combining the rate laws for the three mechanisms identified above, we obtain the rate law given in *Eqn. 8,*

$$-\mathrm{d}[aci\text{-}\mathbf{1}]_t/\mathrm{d}t = (k_0' + k_{H^+}'[H^+])\,[\mathbf{1}^-] + k_{H^+}[H^+][aci\text{-}\mathbf{1}] \qquad (8)$$

where $[aci\text{-}\mathbf{1}]_t = [aci\text{-}\mathbf{1}] + [\mathbf{1}^-]$ is the total concentration of the *aci*-nitro tautomer, k_0' is the rate constant for C-protonation of $\mathbf{1}^-$ by water, k_H^+ is the observed rate constant for the acid-catalyzed reaction of *aci*-**1** yielding **3**, and k_{H^+}' is the rate constant for C-protonation of $\mathbf{1}^-$. The variables $[\mathbf{1}^-]$ and $[aci\text{-}\mathbf{1}]$ can be replaced by means of the ionization quotient of *aci*-**1**, $K_{a,c} = [H^+]\,[\mathbf{1}^-]/[aci\text{-}\mathbf{1}]$ to express the dependence of the observed rate constant on $[H^+]$ in terms of k_0', k_{H^+}, k_{H^+}', and K_a (see *Eqn. 1* in *Sect. 2*). The solid line in *Fig. 3* was obtained by nonlinear least-squares fitting of *Eqn. 1* to the experimental data (*Table 2*). The resulting rate constants k_0', k_{H^+}, and k_{H^+}' and the ionization quotient $K_{a,c}$ of *aci*-**1** are collected in *Table 3*.

The tautomerization constant $K_T = [aci\text{-}\mathbf{1}]/[\mathbf{1}]$ is now defined by the thermodynamic cycle shown in *Scheme 4:* $pK_T = pK_a(\mathbf{1}) - pK_a(aci\text{-}\mathbf{1}) = (20.6 \pm 0.2) - (3.57 \pm 0.02) = 17.0 \pm 0.2$. Density functional calculations predict $pK_T(298\ K) = 20.4$ at the B3LYP/6-311 + G(2d,p)//B3LYP/6-31G(d) level of theory [14].

Buffer Catalysis. In buffer solutions, the decay of $\mathbf{1}^-$ increases with buffer concentration. Bimolecular rate coefficients, k_{buffer}, for buffer catalysis were obtained

Scheme 4

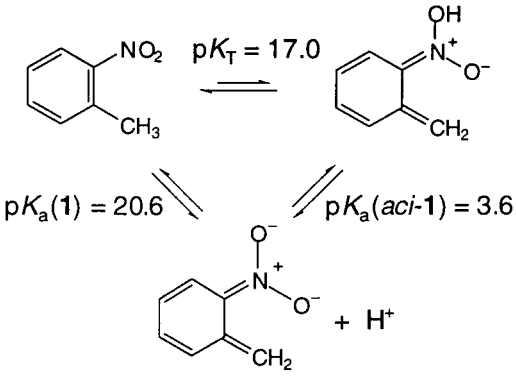

from the slope of the linear increase of observed rate constants with increasing buffer concentration at constant buffer ratio (*Table 2*). Catalysis by the buffers must arise from their general acid components, because the reaction is not accelerated by hydroxy ions, the strongest possible base in aqueous solution (*Fig. 3*). The coefficients k_{buffer} obtained with various buffer ratios should, therefore, be directly proportional to the mol fraction of the acidic buffer component, $x_{HA} = [HA]/([HA] + [A^-])$. However, a plot of the coefficients k_{buffer} obtained with AcOH buffer against x_{HA} was nonlinear. This is due to variation of the ionization ratio of *aci*-**1** in the pH region covered by the AcOH buffers of different composition. General acid catalysis is due to C-protonation of the anion $\mathbf{1}^-$ by the general acid in the rate-determining step. As the ionization equilibrium of *aci*-**1** is established rapidly, the buffer term in the rate law for the observed disappearance of $[aci\text{-}\mathbf{1}]_t = [aci\text{-}\mathbf{1}] + [\mathbf{1}^-]$ may be expressed by the right-hand term in *Eqn. 9*. The observed slopes k_{buffer} of the AcOH buffers (*Table 2*) were, therefore, corrected to account for the variable ionization ratio of *aci*-**1** in these buffers (see *Eqn. 10*), by means of $K_{a,c} = 2.7 \cdot 10^{-4}$ M for the ionization quotient of *aci*-**1** at ionic strength $I = 0.1$M.

$$-\mathrm{d}[aci\text{-}\mathbf{1}]_t/\mathrm{d}t = (k'_{HA}\ [\mathbf{1}^-][HA] = k'_{HA}\{K_a/(K_a + [H^+])\}\ [\text{aci-}\mathbf{1}]_t\ [HA] \tag{9}$$

$$k_{corr} = k_{obs}\ \{(K_a + [H^+])/K_a\} \tag{10}$$

The coefficients k_{corr} thus obtained with the AcOH buffers, and the uncorrected values k_{obs} obtained with the phosphate buffers were linearly related to the mole fraction of the acidic buffer component, $x_{HA} = [HA]/([HA] + [A^-])$. The rate coefficients for the acidic and basic components of the buffer, k'_{HA} and k'_{A^-} (the intercepts for $x_{HA} = 1$ and $x_{HA} = 0$), were determined by nonlinear fitting to $\log\{k_{buffer}/(\mathrm{M}^{-1}\,\mathrm{s}^{-1})\}$ to account for the fact that the standard errors of the slopes k_{corr} or k_{buffer} are proportional to their absolute values. The AcOH buffer showed catalysis of the acidic component only, *i.e.* the intercept at $x_{HA} = 0$ was zero within experimental error. In the case of the phosphate buffer, a small catalytic coefficient was obtained for the formally basic component HPO_4^{2-}, which appears to act as a weak general acid. The following coefficients for

general acid catalysis were obtained: $k'_{HAc} = (1963 \pm 70)$ M^{-1} s^{-1}, $k'_{HPO_4^{2-}} = (34.6 \pm 3.7)$ M^{-1} s^{-1}, and $k'_{H_2PO_4^-} = (310 \pm 7)$ M^{-1} s^{-1}. A *Brønsted* plot of these coefficients including those for water (k'_0) and protons (k'_{H^+}) is shown in *Fig. 4*.

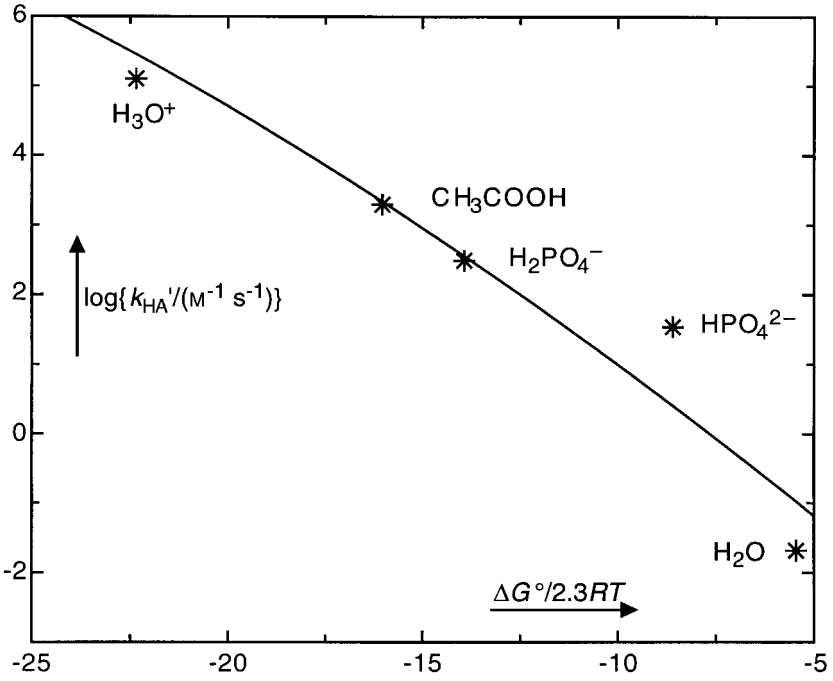

Fig. 4. Brønsted *Plot of the protonation of* **1**$^-$

From these data, the intrinsic free-energy barrier for C-protonation, $\Delta G_0^{\neq}$, can be estimated by the *Marcus* equation (*Eqn. 11*) [41], in which $\Delta G^\circ/(2.3RT) = pK_a$(general acid) $- pK_a$(**1**); k_{diff} was assumed to be 10^{11} M^{-1} s^{-1}. The solid line in *Fig. 4* was obtained by nonlinear last-squares fitting of *Eqn. 11*, giving an intrinsic barrier of $\Delta G_0^{\neq} \approx 34$ kJ mol^{-1}. The intrinsic barrier for C-protonation of enols was determined as 57 kJ mol^{-1} from a more extensive data set [42].

$$k = k_{diff} \exp(-\Delta G^{\neq}/RT), \text{ where } \Delta G^{\neq} = \Delta G_0^{\neq}\ [\Delta G^\circ/(4\Delta G_0^{\neq})]^2 \qquad (11)$$

Nonaqueous Solutions. It is striking that retautomerization of *aci*-**1** is slower in MeOH and MeCN than in H_2O, whereas protonation of **1**$^-$ is faster in these solvents (*Table 4*). These observations can be attributed to medium effects. The acidity constants of C-acids and phenols in MeOH are generally 4–6 units higher than in H_2O [43]. For instance, the dissociation constants of substituted benzoic acids in MeCN are in the range of 16–21 [44], those of nitrophenols in the range of 20–22 [45]. The reaction rate in the acidic plateau will be limited by the ionization constant of *aci*-**1**, $k_{obs} = k'_{H^+}\ K_a$. Therefore, a lower ionization constant K_a leads to a lower level of the acidic plateau, $k_{obs} = 1.4$ s^{-1} (region c in H_2O).

On the other hand, the basic plateau in MeOH is higher than in H_2O (region a) and also higher than region c in MeOH, $k_{obs} = 5.3 \cdot 10^2\ s^{-1}$. For comparison, we measured the reketonization rate constants of acetophenone enol [46] in 0.01M NaOH solutions of H_2O, MeOH, and MeCN. The results show that the enolate ketonizes faster in 10^{-2} M NaOH/MeOH ($8 \cdot 10^4\ s^{-1}$) and in 10^{-2} M NaOH/MeCN ($1.72 \cdot 10^4\ s^{-1}$) than in 10^{-2} M NaOH/H_2O ($7 \cdot 10^3\ s^{-1}$). The same medium effect is operating.

Intramolecular retautomerization of *aci*-**1** to **1** was shown not to be competitive with proton transfer through the solvent in aqueous media. In many nonaqueous solvents, however, a fast component of *aci*-**1** decay is observed, which is attributed to intramolecular proton transfer from the (*Z*)-isomer of *aci*-**1**. The ratio of the amplitudes of the fast and slow transients varied between 0.4 and 1.

The solvent dependence of the rate constants for intramolecular 1,5-H-transfer from O to C in the photoenol of 2-methylacetophenone has been investigated in detail [47]. These rate constants were found to decrease markedly in H-bond accepting solvents. The effect was attributed to a stabilization of the enol by H-bonding. Such dependence was not observed for the decay of the fast transient (*Z*)-*aci*-**1**. In polar solvents, deprotonation and (*Z*) → (*E*) isomerization at the nitronic acid compete with the intramolecular reaction. Calculations predict (*Z*)-*aci*-**1** to be *ca.* 17 kJ mol^{-1} less stable than (*E*)-*aci*-**1** which implies essentially complete conversion to (*E*)-*aci*-**1** [14]. In fact, we observed no fast transient in aqueous or basic alcoholic solutions. The observed kinetic isotope effect of D_7-**1** for the fast transient in hexane (1.87 ± 0.14) indicates that intramolecular proton transfer is the dominant decay process in this solvent.

Comparison with Aliphatic and Polynitroaromatic aci-*Nitro Compounds.* Rearomatization provides a driving force that lowers the tautomerization constants of 2-nitrobenzyl derivatives relative to those of aliphatic nitro compounds by 10–15 orders of magnitude (see *Table 6*). The rate coefficient for the acid-catalyzed *Nef*-type reaction of *aci*-**1**, $k_{H^+} = (2.47 \pm 0.05)\ M^{-1}\ s^{-1}$ in aqueous solution, is about two orders of magnitude higher than that of aliphatic nitro compounds (2-nitropropane: $(1.30 \pm 0.13) \cdot 10^{-2}\ M^{-1}\ s^{-1}$; nitrocyclohexane $(1.48 \pm 0.08) \cdot 10^{-1}\ M^{-1}\ s^{-1}$ in 80% MeOH/H_2O at 0° [34]). The rate constant observed for these reactions, $k_{obs} = k_0/K_a$, is determined by both the rate constant of hydration k_0 and the acidity constant K_a of the diprotonated *aci*-species. Resonance-stabilized *aci*-nitroalkanes like α-phenylnitroethane [57] and phenylnitromethane [58] do not or very slowly undergo the *Nef* reaction, and retautomerization dominates. Due to the electron-withdrawing effect of the nitro groups, polyaromatic compounds show smaller acidity constants of the Me groups as well as of their *aci*-tautomers. Taken together, these opposing effects result in similar tautomerization constants for mono- and polynitroaromatic derivatives (*Table 6*).

Experimental Part

Materials. The 2-nitrotoluene (**1**; *Fluka, p.a.*) was purified twice by crystallization from hexane that was slowly cooled to −50° in dry ice/acetone. Bidistilled H_2O was used to prepare aq. solns. Other solvents of spectroscopic grade were used as received. Hexamethylphosphoramide (HMPA; *Aldrich*, 99%) was distilled from BaO under reduced pressure (20 mbar).

2-Nitro(D$_7$)toluene (D_7-**1**). According to [59], (D_8) toluene (5 ml) and Ac_2O (25 ml) were cooled to +5°. A mixture of DNO_3 (68%; 2.2 ml) and CH_3COOD (5.6 ml) was slowly added so that the temp. remained in the

Table 6. *Thermodynamic and Kinetic Parameters of* aci-*Nitro Tautomerization*

	pK_a (nitro)	pK_a (aci)	pK_T	$k_{HO^-}/(M^{-1}\,s^{-1})$	$k'_{H^+}/(M^{-1}\,s^{-1})$	k'_0/s^{-1}
Aromatic compounds:						
2-nitrotoluene[a])	20.6	3.57	17.0	$1.8\cdot10^{-7}$	$1.26\cdot10^{5}$	1.16
2,4-dinitrotoluene[b])	17.12[c])	1.1	16.12		$7.4\cdot10^{4}$	1.0
2,6-dinitrotoluene[d])	19	1.8	17.2		$1\cdot10^{5}$	0.95
2,4,6-trinitrotoluene[c,e])	14.45	<-0.12[a])	>15		$8.67\cdot10^{4}$[a])	1.30[a])
Aliphatic compounds:						
nitromethane	10.21[f])	3.25[g])	7.03	26.6[h])	715[i]), 683[j])	
nitroethane	8.44[f])	4.41[f])	4.04	5.19[h])	15[j])	
1-nitropropane[j])	8.98[k])	4.6	4.38	3.25	75	
2-nitropropane	7.68[f])	5.11[f])	2.56	0.355[l])		
phenylnitromethane[j])	6.8	3.9	2.9	0.317[h])	317	
dinitromethane[j])	3.57	1.86	1.7	0.83	3167	

[a]) This work. [b]) 30° [7]. [c]) [48]. [d]) 30° [8]. [e]) [49]. [f]) [50]. [g]) 0° [51]. [h]) [52]. [i]) [53]. [j]) [54]. [k]) [55]. [l]) [56].

range of 5–10°. The mixture was stirred for 2 h at r.t., then D_2O (50 ml) was added. The org. compounds were extracted with Et_2O (3×50 ml). The combined org. phase was washed with heavy water, dried (Na_2CO_3), and evaporated. Distillation under reduced pressure gave a mixture (4.5 g, 60%) of 2- (74%), 3- (3%), and 4-nitro(D_7)toluene (23%) according to GC/MS. A sample (0.2 g) of this mixture was separated by HPLC yielding 0.12 g of 2-nitro(D_7)toluene (isotopic purity > 95% by GC/MS). EI-MS (*m*/*z*, rel.%): 52 (10.2), 53 (0.7), 54 (13.4), 55 (0.7), 56 (3.6), 58 (2.6), 62 (2.3), 64 (6.4), 66 (19.0), 67 (1.2), 68 (6.0), 70 (83.7), 71 (4.8), 72 (1.0), 74 (0.4), 76 (2.8), 78 (1.8), 80 (1.3), 82 (22.2), 83 (3.2), 84 (4.0), 85 (1.4), 86 (4.0), 87 (0.3), 88 (0.8), 90 (0.5), 94 (15.0), 95 (1.5), 96 (8.8), 98 (100), 99 (7.5), 100 (1.7), 110 (0.8), 114 (1.1), 126 (75.7), 127 (6.3), 128 (0.8), 144 (12.1), 145 (1.0).

Methods. The equipment used for flash photolysis has been described previously [60]. Reaction kinetics were determined by excitation with either 20-μs pulses from a conventional electric discharge lamp of up to 1000 J electrical energy or by 25-ns pulses from an excimer laser (248, 308, or 351 nm, pulse energies up to 200 mJ). A calibrated *Joulemeter ED-500*, *Gentec*, Canada, was used to determine pulse energies. Subpicosecond laser pulses at 248 nm were used to follow the formation of *aci*-**1** by pump-probe spectroscopy. The kinetic data for the pH-rate profile were obtained at $25.0\pm0.1°$ with aq. solns. of **1** ($1-5\cdot10^{-4}$ M).

Quantum yields were determined by spectrophotometric monitoring of the reaction progress with the aid of azobenzene actinometry [61]. To determine the kinetics of base-catalyzed D-exchange in 2-nitrotoluene, solns. of **1** ($4\cdot10^{-4}$ M) in 20 ml of 1.0M NaOD in D_2O were kept in the dark at $25\pm0.1°$ for several days and then extracted with CH_2Cl_2. The org. phase was dried (Na_2SO_4) and evaporated, and the amount of D-exchange of **1** (10–23% conversion) was determined by GC/MS analysis. Prior to isotope exchange, the $[M+1]^+$ peak of **1** had 8 ± 1% the intensity of the molecular-ion peak M^+, as expected for the natural isotope distribution. Both the $[M-1]^+$ and the $[M+2]^+$ peaks were of negligible intensity in all spectra, so that the amount of deuteration could be calculated from the simple formula of *Eqn. 12* where $x=I_{[M+1]^+}/I_{M^+}$ is the ratio of the observed peak intensities of the $[M+1]^+$ and M^+ signals. Reaction times/h (NaOD concentration/M, *x*): 137 (1.03, 0.219), 285 (1.00, 0.374), 79 (1.00, 0.204).

$$[D_1\text{-}\mathbf{1}]/[\mathbf{1}]=(x-0.08)/(1+x-0.08) \tag{12}$$

This work was supported by the *Swiss National Science Foundation*, project 20-53919.98. We thank Dr. *Svetlana V. Kombarova*, Basel, for the synthesis of D_7-**1**.

REFERENCES

[1] T. W. Greene, P. G. M. Wuts, 'Protective Groups in Organic Synthesis', 2nd edn., Wiley, New York, 1991.
[2] F. M. Houlihan, O. Nalamasu, J. M. Kometani, E. Reichmanis, *J. Imaging Sci. Technol.* **1997**, *41*, 35.
[3] J. E. T. Corrie, D. R. Trentham, in 'Bioorganic Photochemistry', Vol. 2, 'Biological Applications of Photochemical Switches', Ed. H. Morrison, Wiley, New York, 1993, pp. 243–305.

[4] 'Methods in Enzymology', Vol. 291, 'Caged Compounds', Ed. G. Marriott, Academic Press, New York, 1998, and ref. cit. therein.
[5] J. D. Margerum, L. J. Miller, in 'Techniques of Chemistry', Vol. III, 'Photochromism', Ed. G. H. Brown, Wiley-Interscience, New York, 1971, p. 580.
[6] G. Wettermark, *J. Phys. Chem*. **1962**, *66*, 2560; G. Wettermark, E. Black, L. Dogliotti, *Photochem. Photobiol*. **1965**, *4*, 229.
[7] G. Wettermark, R. Ricci, *J. Chem. Phys.* **1963**, *39*, 1218.
[8] M. E. Langmuir, L. Dogliotti, E. D. Black, G. Wettermark, *J. Am. Chem. Soc*. **1969**, *91*, 2204.
[9] K. Suryanarayanan, C. Capellos, *Int. J. Chem. Kinet*. **1974**, *6*, 89.
[10] J. A. Sousa, J. Weinstein, *J. Org. Chem*. **1962**, *27*, 3155.
[11] H. Sixl, R. Warta, *Chem. Phys.* **1985**, *94*, 147.
[12] A. Barth, J. E. T. Corrie, M. J. Gradwell, Y. Maeda, W. Mäntele, T. Meier, D. R. Trentham, *J. Am. Chem. Soc*. **1997**, *119*, 4149.
[13] J. A. McCray, N. Fidler-Lim, G. C. R. Ellis-Davies, J. H. Kaplan, *Biochemistry* **1992**, *31*, 8856.
[14] Y. V. Il'ichev, J. Wirz, *J. Phys. Chem. A* **2000**, 7856.
[15] H. Morrison, B. H. Migdalof, *J. Org. Chem*. **1965**, *30*, 3996.
[16] A. J. Kresge, H. J. Chen, G. L. Kapen, M. F. Powell, *Can. J. Chem*. **1983**, *61*, 249.
[17] R. G. Bates, 'Determination of pH. Theory and Practice', Wiley, New York, 1973.
[18] H. S. Harned, R. W. Ehlers, *J. Am. Chem. Soc*. **1933**, *55*, 652.
[19] A. K. Grzybowski, *J. Phys. Chem*. **1958**, *62*, 555.
[20] V. Gold, S. Christ, *J. Chem. Soc., Perkin Trans. 2* **1972**, 89.
[21] A. J. Kresge, *Can. J. Chem.* **1974**, *52*, 1897.
[22] J. L. Lelievre, P. G. Farrell, F. Terrier, *J. Chem. Soc.*, *Perkin Trans. 2* **1986**, 333.
[23] J. D. Margerum, C. T. Petrusis, *J. Am. Chem. Soc*. **1969**, *91*, 2467.
[24] M. S. Simmons, R. G. Zepp, *Water Res.* **1986**, *20*, 899.
[25] R. Hurley, A. C. Testa, *J. Am. Chem. Soc*. **1968**, *90*, 1949.
[26] M. Takezaki, N. Hirota, M. Terazima, *J. Phys. Chem. A* **1997**, *101*, 3443.
[27] M. Takezaki, N. Hirota, M. Terazima, *J. Chem. Phys.* **1998**, *108*, 4685.
[28] R. W. Yip, D. K. Sharma, R. Giasson, D. Gravel, *J. Phys. Chem*. **1984**, *88*, 5770; R. W. Yip, D. K. Sharma, R. Giasson, D. Gravel, *J. Phys. Chem*. **1985**, *89*, 5328; R. W. Yip, D. K. Sharma, R. Giasson, D. Gravel, Y. X. Wen, *J. Phys. Chem.* **1991**, *95*, 6078; R. W. Yip, D. K. Sharma, R. Giasson, D. Gravel, D. Blanchet, *Can. J. Chem*. **1991**, *69*, 1193.
[29] W. M. Nau, G. Greiner, H. Rau, J. Wall, M. Olivucci, J. C. Scaiano, *J. Phys. Chem. A* **1999**, *103*, 1579.
[30] G. M. Loudon, *J. Chem. Educ.* **1991**, *68*, 973.
[31] J. Wirz, *Chem. unserer Zeit* **1998**, *32*, 311.
[32] R. P. Bell, 'The Proton in Chemistry', Cornell University Press, Ithaca, 1959, p. 188.
[33] F. G. Bordwell, W. J. Boyle, *J. Am. Chem. Soc*. **1975**, *97*, 3447.
[34] M. F. Hawthorne, *J. Am. Chem. Soc*. **1957**, *79*, 2510.
[35] N. Kornblum, R. A. Brown, *J. Am. Chem. Soc.* **1965**, *87*, 1742.
[36] S. F. Sun, J. T. Folliard, *Tetrahedron* **1971**, *27*, 323.
[37] J. T. Edward, P. H. Tremaine, *Can. J. Chem*. **1971**, *49*, 3493.
[38] R. B. Cundall, A. W. Locke, *J. Chem. Soc. B* **1968**, 98.
[39] T. Ohwada, N. Yamagata, K. Shudo, *J. Am. Chem. Soc*. **1991**, *113*, 1364.
[40] W. Grünbein, A. Fojtik, A. Henglein, *Monatsh. Chem*. **1970**, *101*, 1243.
[41] A. O. Cohen, R. A. Marcus, *J. Phys. Chem*. **1968**, *72*, 4249.
[42] J. Wirz, *Pure Appl. Chem*. **1998**, *70*, 2221.
[43] F. Rived, M. Roses, E. Bosch, *Anal. Chim. Acta* **1998**, *374*, 309.
[44] I. M. Kolthoff, M. K. Chantooni, Jr., *J. Am. Chem. Soc*. **1970**, *92*, 7025; I. M. Kolthoff, M. K. Chantooni, Jr., *J. Phys. Chem*. **1966**, *70*, 856.
[45] I. M. Kolthoff, M. K. Chantooni, Jr., S. Bhowmik, *J. Am. Chem. Soc*. **1966**, *88*, 5430.
[46] P. Haspra, S. Sutter, J. Wirz, *Angew. Chem*. **1979**, *18*, 617; Y. Chiang, A. J. Kresge, J. Wirz, *J. Am. Chem. Soc*. **1984**, *106*, 6392.
[47] R. Haag, J. Wirz, *Helv. Chim. Acta* **1977**, *60*, 2595.
[48] R. Schaal, *Bull. Soc. Chim. Fr.* **1954**, 1036.
[49] R. Schaal, *J. Chim. Phys.* **1955**, *52*, 796.
[50] D. Turnbull, S. H. Maron, *J. Am. Chem. Soc*. **1943**, *65*, 212.

[51] R. Junell, Dissertation, Upsala, Sweden, 1935.
[52] R. P. Bell, D. M. Goodall, *Proc. R. Soc. London A* **1966**, *294*, 273.
[53] I. Erden, J. R. Keefe, F.-P. Xu, J.-B. Zheng, *J. Am. Chem. Soc*. **1993**, *115*, 9834.
[54] A. T. Neilson, in 'The Chemistry of the Nitro and Nitroso Groups', Part 1, Ed. H. Feuer, Wiley, London, 1969, p. 350.
[55] G. W. Wheland, J. Farr, *J. Am. Chem. Soc*. **1943**, *65*, 1433.
[56] A. J. Kresge, D. Drake, Y. Chiang, *Can. J. Chem*. **1974**, *52*, 1889.
[57] E. Bamberger, R. Seligman, *Chem. Ber.* **1903**, *36*, 701.
[58] N. Kornblum, G. E. Graham, *J. Am. Chem. Soc*. **1951**, *73*, 4041.
[59] S. M. Lee, J. M. Roseman, C. B. Zartman, E. P. Morrison, S. J. Harrison, *J. Fluorine Chem*. **1996**, *77*, 65.
[60] E. Hasler, A. Hörmann, G. Persy, J. Wirz, *J. Am. Chem. Soc*. **1993**, *115*, 5400.
[61] G. Gauglitz, S. Hubig, *Z. Phys. Chem., N. F.* **1984**, *139*, 237; G. Gauglitz, S. Hubig, *J. Photochem*. **1985**, *30*, 121; G. Persy, J. Wirz, *EPA Newslett*. **1987**, *29*, 45.

Received April 2, 2001